

See discussions, stats, and author profiles for this publication at: <https://www.researchgate.net/publication/7961953>

Phase Behavior of the Lecithin/Water/Isooctane and Lecithin/Water/Decane Systems

ARTICLE *in* LANGMUIR · FEBRUARY 2004

Impact Factor: 4.46 · DOI: 10.1021/la035603d · Source: PubMed

CITATIONS

42

READS

66

6 AUTHORS, INCLUDING:



Ruggero Angelico

Università degli Studi del Molise

51 PUBLICATIONS 605 CITATIONS

SEE PROFILE



Andrea Ceglie

Università degli Studi del Molise

121 PUBLICATIONS 1,845 CITATIONS

SEE PROFILE



Giuseppe Colafemmina

Università degli Studi di Bari Aldo Moro

55 PUBLICATIONS 849 CITATIONS

SEE PROFILE



Gerardo Palazzo

Università degli Studi di Bari Aldo Moro

154 PUBLICATIONS 2,027 CITATIONS

SEE PROFILE

Phase Behavior of the Lecithin/Water/Isooctane and Lecithin/Water/Decane Systems

Ruggero Angelico,[†] Andrea Ceglie,[†] Giuseppe Colafemmina,^{†,‡} Fabio Delfino,[‡] Ulf Olsson,[§] and Gerardo Palazzo^{*,†,‡}

DISTAAM, Università del Molise, v. De Sanctis, I-861 00 Campobasso, Italy, Physical Chemistry 1, Center for Chemistry and Chemical Engineering, Lund University, P.O. Box 124, S-221 00 Lund, Sweden, and Dipartimento di Chimica, Università di Bari, v. Orabona 4, I-70126 Bari, Italy

Received August 28, 2003. In Final Form: November 4, 2003

The isothermal pseudo-ternary-phase diagram was determined at 25 °C for systems composed of lecithin, water, and, as oil, either isooctane or decane. This was accomplished by a combination of polarizing microscopy, small-angle X-ray scattering, and NMR techniques. The lecithin-rich region of the phase diagram is dominated by a lamellar liquid-crystalline phase (L_α). For lecithin contents less than 60% and low hydration (mole ratio water/lecithin = $W_0 < 5.5$), the system forms a viscous gel of branched cylindrical reverse micelles. With increase in the water content, the system phase separates into two phases, which is either gel in equilibrium with essentially pure isooctane (for lecithin $< 25\%$) or a gel in equilibrium with L_α (for lecithin $> 25\%$). These two-phase regions are very thin with respect to water dilution. For $8 < W_0 < 54$ very stable water-in-oil emulsions form. It is only after ripening for more than 1 year that the large region occupied by the emulsion reveals a complex pattern of stable phases. Moving along water dilution lines, one finds (i) the coexistence of gel, isooctane and L_α , (ii) equilibrium between reverse micelles and spherulites, and, finally, (iii) disconnected reverse micelles that fail to solubilize water for $W_0 > 54$. This results in a Winsor II phase equilibrium at low lecithin content, while for lecithin $> 20\%$ the neat water is in equilibrium with a reverse hexagonal phase and an isotropic liquid-crystalline phase. The use of the decane as oil does not change the main features of the phase behavior.

1. Introduction

Lecithin (1,2-diacyl-*sn*-glycero-3-phosphocholine) is a natural phospholipid that in most organisms accounts for more than 50% of the lipid matrix of biological membranes. The phase behavior of lecithin, water, and oils is of great interest for several reasons. In the water-rich region it should reflect the effect of hydrophobic molecules on lipid bilayers, a topic relevant for the comprehension of the mechanism of general anesthesia and for some environmental health aspects.¹ Since lecithin is a fully biocompatible substance, it is widely used in every day life as surfactant, and mixtures of lecithin, water, and oils are adopted in human and animal food, medicine, cosmetics, and pharmaceuticals.²

The water-lean region has been the subject of several investigations as well. Previous scattering investigations demonstrated that lecithin reverse micelles in many nonpolar solvents form giant cylindrical reverse micelles upon addition of small water amounts.³ At constant lecithin concentration, with increasing water loading, these tubular reverse micelles entangle, thus forming a transient network with viscoelastic properties. Macroscopically, the system appears as a viscous gel, often termed an *organogel*.⁴ Microscopically, the length distribution of wormlike reverse micelles is expected to vary

reversibly with lecithin concentration, water content, temperature, and shear in agreement with theories developed for *living polymers*.⁵ The gel is thermostable, thermoreversible, and isotropic. If the viscosity of the organogel is measured versus water addition, a maximum viscosity is reached at a given hydration level that strongly depends on the organic solvent.⁴ Further hydration results in a gradual decrease in viscosity until a phase separation is attained. Lecithin organogels made with suitable oils have also been proposed to deliver pharmaceuticals.^{6–8} In general, the role of the self-assembled microstructures in the macroscopic gel formation remains a particularly challenging question. Lecithin organogels are nonionic oil-continuous systems where complications due to electrostatic interactions are avoided. Moreover, their structural relaxation after mechanical deformation can be long (of the order of an hour) and can be conveniently investigated by various techniques.^{9,10} For these reasons, lecithin organogels represent a suitable model system of living polymers⁵ despite the heterogeneity in chain composition of the lecithin extracted from soybean.

Although the formation of lecithin organogel has been reported for about 50 different organic solvents,¹¹ struc-

* To whom correspondence may be addressed. E-mail: palazzo@chimica.uniba.it.

[†] DISTAAM, Università del Molise.

[‡] Dipartimento di Chimica, Università di Bari.

[§] Physical Chemistry 1, Center for Chemistry and Chemical Engineering, Lund University.

(1) Larsson, K. *Langmuir* **1988**, *4*, 215 and references therein.

(2) Wendel, A. In *Encyclopedia of Chemical Technology*; Kirk, R. E., Othmer, D. F., Eds.; John Wiley & Sons: New York, 1995; Vol. 15, p 192.

(3) Schurtenberger, P.; Jerke, G.; Cavaco, C.; Pedersen, J. S. *Langmuir* **1996**, *12*, 2433 and references therein.

(4) Scartazzini, R.; Luisi, P. L. *J. Phys. Chem.* **1989**, *92*, 829.

(5) Cates, M. E.; Candau, S. J. *J. Phys.: Condens. Matter* **1990**, *2*, 6869 and references therein.

(6) Papanoniotou, I.; Müller-Goymann, C. C. *Pharm. Pharmacol. Lett.* **1995**, *5*, 28.

(7) Müller-Goymann, C. C.; Hamann, H. J. *J. Controlled Release* **1993**, *23*, 165.

(8) Mackeben, S.; Müller, M.; Müller-Goymann, C. C. *Colloids Surf., A* **2001**, *183*, 699.

(9) Angelico, R.; Olsson, U.; Mortensen, K.; Ambrosone, L.; Palazzo, G.; Ceglie, A. *J. Phys. Chem. B* **2002**, *106*, 2426.

(10) Angelico, A.; Burgemeister, D.; Ceglie, A.; Olsson, U.; Palazzo, G.; Schmidt, C. *J. Phys. Chem. B* **2003**, *107*, 10325.

(11) Luisi, P. L.; Scartazzini, R.; Haering, G.; Schurtenberger, P. *Colloid Polym. Sci.* **1990**, *268*, 356.

tural investigations have only been performed on systems based on three oils, viz., cyclohexane (cC_6), isooctane (iC_8), and decane (C_{10}); for reviews see refs 12–14. Further insights on the above-reported studies, require quantitative characterizations of the whole phase diagram. Apart from a few and incomplete studies of the phase behavior of diluted^{15,16} and concentrated¹⁷ lecithin/water/oil mixtures, a complete phase diagram investigation was reported only in the case of the lecithin/water/cyclohexane system.¹⁸ In the present study we extend that phase behavior study to the lecithin/water/isooctane and lecithin/water/decane systems.

2. Materials and Methods

Soybean lecithin (Epikuron 200) was a generous gift from Degussa Bioactives AG and consists of soybean *phosphatidylcholine* (PC) with a purity of 95% and with an average molecular weight of 772. The lecithin used in this work is of the same brand used in most of the published investigations of this system, and as in previous work, it was used without further purification which consequently means that it is a certain mixture of phosphatidylcholines of different chain lengths and degree of saturation.¹⁹ Isooctane (2,2,4-trimethylpentane) of purity >99.0% was obtained from Carlo Erba, Italy; decane (puriss. grade) was obtained from Fluka Chemie AG, Switzerland; water was twice-distilled in an all-quartz device. To allow for 2H NMR measurements, some samples were prepared with D_2O (99.80 atom % 2H , purchased from Dr. Glaser AG, Switzerland). All the chemicals were used as received.

Microscopy with polarized optics, small-angle X-ray scattering (SAXS), and 1H and 2H NMR measurements were performed as described in ref 18. The measurements of water and lecithin self-diffusion coefficients via pulsed gradient spin-echo (PGSE) NMR was achieved by using the apparatus described elsewhere.²⁰

The samples were prepared by weighing appropriate amounts of lecithin, water, and oil into glass tubes with screw caps. The samples were mixed by repeated centrifugation or shaking (depending on their stiffness) at regular intervals for 2–3 weeks. Then, they were allowed to stand for almost 3 weeks at 25.0 ± 0.2 °C in a water bath thermostat. Selected samples were allowed to ripen for more than 1 year; in such a case they were stored in a room at 25 ± 4 °C for most of the time and finally allowed to stand in the water bath for 4 weeks. All the samples were kept in the dark to minimize the lecithin photooxidation.

The phase behavior is here presented in weight fraction in a triangular Gibbs representation, with lecithin, H_2O , and oil as the corners of the triangle. Samples prepared with heavy water were also included in the diagrams by taking into account the difference in molecular weight between H_2O and D_2O .

For samples showing macroscopic phase separation, the volume fraction of the different phases was recorded and the composition of the liquid phases was measured by 1H NMR spectroscopy. This was accomplished by comparing the areas of the NMR peaks characteristic of water and lecithin (trimethylammonium resonance) with the area of the NMR signal of benzene added as internal standard. When a liquid crystalline phase was present, its composition was evaluated from the

difference between the overall composition and the composition of the liquid phases.

As a final *caveat*, it should be stressed that in the case of multiphase regions the boundaries have been drawn under the assumption of a pseudoternary behavior. Soybean lecithin is strictly a multicomponent mixture, and deviation from the pseudoternary behavior is expected; however the self-consistency of the results obtained suggest the multicomponent nature of the surfactant has a negligible influence on the phase diagram (the same is not true for the rheological behavior, as demonstrated in ref 21).

To conclude this section we present the notation and numerical parameters used within this paper. The following notation will be used for the sake of shortness: W_0 = mole ratio water/lecithin; lecithin = PC; isooctane = iC_8 ; decane = C_{10} ; cyclohexane = cC_6 ; H_2 = reverse hexagonal phase; L_α = lamellar phase; I = cubic phase; L_2 = microemulsion phase made of disconnected reverse micelles (regardless if spherical or not); gel phase = interconnected reverse micelles (see section 3.2); Φ_{PC} , Φ_W , and Φ_{W+PC} are the lecithin volume fraction, the water volume fraction, and the sum of water and lecithin volume fractions, respectively.

In the calculations we have used the following parameters (the primary references can be found elsewhere):¹⁸ $v_w = 30$ Å³ (molecular volume of water); $v_{PC} = 1257$ Å³ (average molecular volume of lecithin); $v_{HG} = 204$ Å³ (volume of the lecithin polar headgroup).

3. Results

Special care must be taken to avoid kinetic artifacts when studying the phase behavior of phospholipid systems. In particular, for the system PC/water/ iC_8 the presence of a region of the phase diagram where the system forms emulsions that are stable for several months was recently reported by us.²² Since this is the time window of interest in most applications and fundamental investigations, we will illustrate first this short-time behavior (section 3.1) and defer to the subsequent section (section 3.2) the equilibrium phase diagram that is attained over a long time scale (more than 1 year). Finally the results concerning the system PC/water/ C_{10} are reported in section 3.3.

3.1. PC/Water/ iC_8 : Short-Time Phase Behavior.

The complete pseudoternary phase map obtained from observations taken over a time window of less than 2 months is presented in weight fractions in Figure 1. It is based on the analysis of about 200 samples. As is well-known, upon the addition of 1–2 mol of water per mole of PC, solutions of lecithin in iC_8 become highly viscoelastic while still remaining transparent and optically isotropic.^{4,23} Notwithstanding the high viscosity (up to 6 orders of magnitude higher than the viscosity of neat iC_8), the system is still a liquid. This is a highly organized liquid, with cylindrical *reverse* micelles as building blocks,¹⁵ often filed as “ L_2 phase”. However, for reasons that will be clarified later (section 3.2), we will refer to such a state as a “gel phase” reserving the classification L_2 phase to more orthodox reverse micelles. The viscosity of such a gel phase depends in a particular way on the water content. When reported as a function of the mole ratio of water/lecithin (hereafter W_0), the viscosity first increases by several orders of magnitude (depending on the PC/ iC_8 ratio), reaches a maximum (located at $W_0 = 2.5$ – 3.0), and then decreases. At extreme dilution (lecithin <0.4 wt %) the system is composed of relatively stiff rodlike micelles.²⁴

(12) Shchipunov, Y. A. *Colloid Surf., A* **2001**, 183–185, 541 and references therein.

(13) Schurtenberger, P. *Chimia* **1994**, 48, 72.

(14) Palazzo, G.; Angelico, R.; Ceglie, A.; Olsson, U. In *Self-Assembly*; Robinson, B., Ed.; IOS Press: Burke, VA, 2003; p 318.

(15) Schurtenberger, P.; Scartazzini, R.; Magid, L. J.; Leser, M. E.; Luisi, P. L. *J. Phys. Chem.* **1990**, 94, 3695.

(16) Schurtenberger, P.; Peng, Q.; Leser, M. E.; Luisi, P. L. *J. Colloid Interface Sci.* **1993**, 156, 43.

(17) Sjölund, M.; Lindblom, G.; Rilfors, L.; Arvidson, G. *Biophys. J.* **1987**, 52, 145.

(18) Angelico, R.; Ceglie, A.; Olsson, U.; Palazzo, G. *Langmuir* **2000**, 16, 2124.

(19) Shinoda, K.; Araki, M.; Sadaghiani, A. S.; Khan, A.; Lindman, B. *J. Phys. Chem.* **1991**, 95, 989.

(20) Giustini, M.; Palazzo, G.; Colafemmina, G.; Della Monica, M.; Giomini, M.; Ceglie, A. *J. Phys. Chem.* **1996**, 100, 3190.

(21) Cirkel, P. A.; Fontana, M.; Koper, G. J. M. *Langmuir* **1999**, 15, 3026.

(22) Stefan, A.; Palazzo, G.; Ceglie, A.; Panzavolta, E.; Hochkoeppler, A. *Biotechnol. Bioeng.* **2003**, 81, 323.

(23) Schurtenberger, P.; Scartazzini, R.; Luisi, P. L. *Rheol. Acta* **1989**, 28, 372.

(24) Cirkel, P. A.; Koper, G. J. M. *Langmuir* **1998**, 14, 7095.

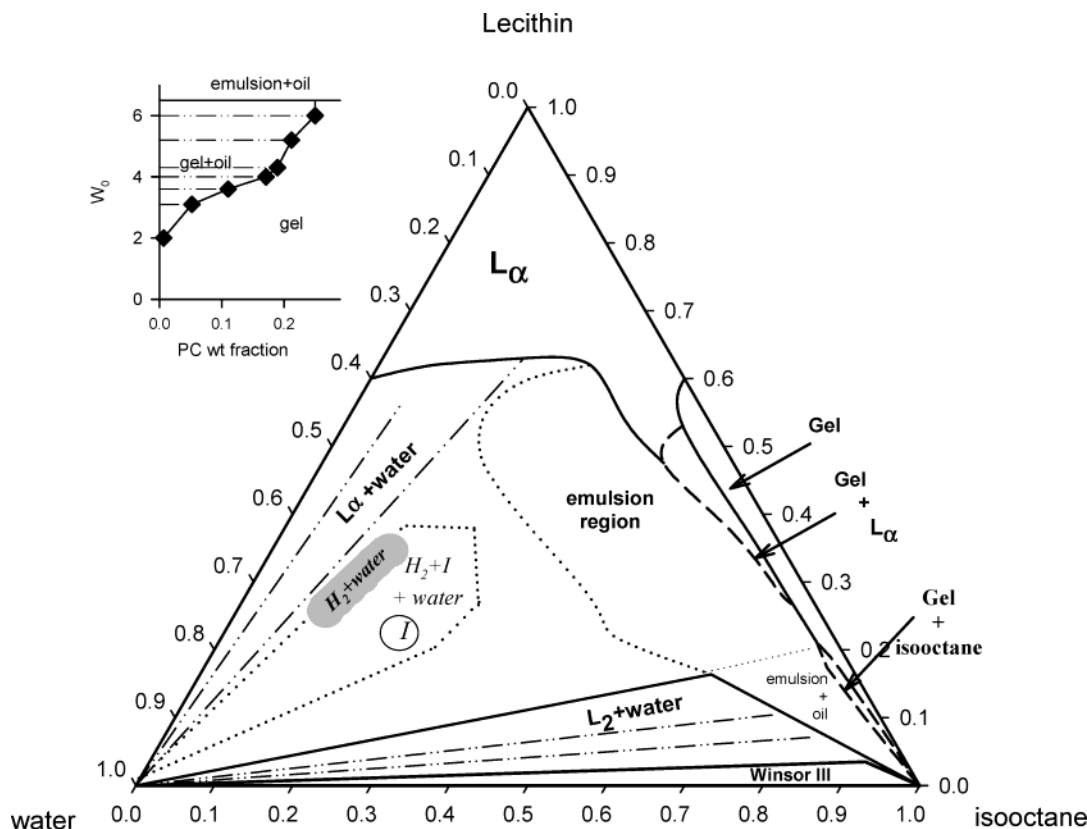


Figure 1. Short-time phase map in weight fraction for the lecithin/water/isooctane system. It was obtained from observations taken over a time window of less than 2 months. The phase abbreviations are as reported in section 2. The $H_2 + I + \text{water}$ region and the emulsion region are shown approximately with dotted lines. Tie lines are denoted by dot–dash. Inset: extension of the gel + isooctane coexistence loop shown as W_0 vs lecithin weight fraction.

However, in the realm of *true* gels (i.e., for lecithin > 0.4 wt %) the microstructure of the system depends dramatically on the water content. With increase of W_0 , wormlike reverse micelles become branched. Dielectric spectroscopy²⁵ and PGSE-NMR²⁶ investigations confirm the presence of branches that accounts for the decrease in viscosity, because the branch points can slide along the micellar contour.²⁷ Moreover, the density of micellar junctions increases with increasing W_0 parameter, and finally the network collapses expelling almost pure isooctane, as predicted by theories on a branched living network (reviewed in section 4.1). As previously reported,¹⁵ the phase boundary between the gel and the gel + isooctane coexistence is not located at a fixed W_0 . W_0 at the boundary slightly increases with the lecithin concentration, from a value of $W_0 = 2.0$ at lecithin content ~ 0.7 wt % to $W_0 = 6.0$ at 25 wt % of lecithin. Since this two-phase region is barely discernible in the triangular representation, we have drawn it also in the Cartesian plot W_0 vs PC weight fraction in the insert of Figure 1.

Moving toward the lecithin corner, the gel phase is in equilibrium with a lamellar phase (L_α). For lecithin concentration higher than 70% the birefringent samples are stiff, and their SAXS spectra are characterized by a sharp first-order Bragg peak followed by weaker reflections at higher q values (Figure 2A). At high lecithin/isooctane ratios, the lamellar phase is stable up to a maximum water

content of about 40% corresponding to $W_0 = 28$; further water loading results in an equilibrium between the lamellar phase and excess water (as also found for the binary water/lecithin system).²⁸

Lamellar samples with less than 70 wt % of lecithin have a semicloudy appearance and are birefringent with a mosaic texture. SAXS spectra show only one narrow principal reflection together with a shoulder at lower q values (Figure 2A). The higher diagnostic reflections were often hardly discernible, but the ^2H NMR spectra show nice quadrupolar splitting (Table 1). Results obtained from SAXS and ^2H NMR measurements on lamellar samples at $W_0 \approx 5$ and different isooctane loading are listed in Table 1.

The repeat distance d , probed by SAXS experiments, is the sum of lipid bilayers, water layer thickness (d_w), and oil layer thickness (d_{oil}). For one-dimensional swelling along oil dilution lines, d depends on the lecithin and water volume fractions according to

$$d = \frac{2L + d_w}{\Phi_{w+PC}} = \frac{2v_{PC} + v_w W_0}{\alpha \Phi_{w+PC}} \quad (1)$$

where L and α are the length and the polar head area, respectively, of a lecithin molecule in the lamellar phase and Φ_{w+PC} is the sum of water and lecithin volume fractions.

As illustrated in Figure 2B, the swelling with oil supports the occurrence of a lamellar phase. A linear fit of the repeat distance to $1/\Phi_{w+PC}$ gives a bilayer *plus* water layer thickness $2L + d_w = 55 \pm 9 \text{ \AA}$, fully consistent with

(25) Cirkel, P. A.; van der Ploeg, J. P. M.; Koper, G. J. M. *Phys. Rev. E* **1998**, *57*, 6875. Cirkel, P. A.; Fontana, M.; Koper, G. J. M. *J. Dispersion Sci. Technol.* **2001**, *2*–3, 211.

(26) Ambrosone, L.; Angelico, R.; Ceglie, A.; Olsson, U.; Palazzo, G. *Langmuir* **2001**, *17*, 6822.

(27) Appel, J.; Porte, G.; Khatory, A.; Kern, F.; Candau, S. J. *J. Phys. II* **1992**, *2*, 1045.

(28) Small, D. M. *J. Lipid Res.* **1967**, *8*, 551.

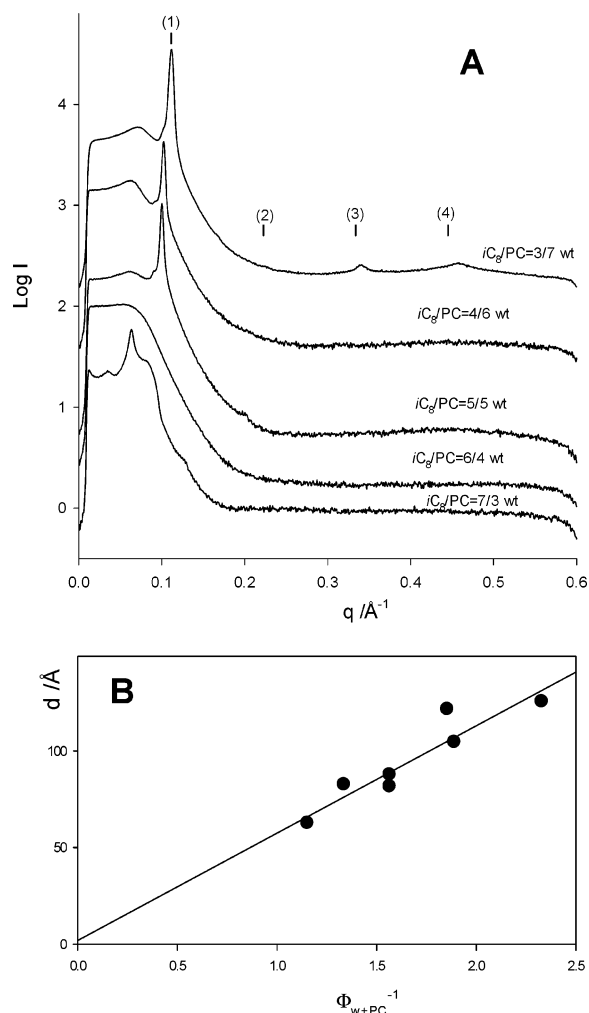


Figure 2. Samples in the L_α region of Figure 1. (A) SAXS diffraction pattern of samples at constant $W_0 = 5.5$ and different isooctane/lecithin mass ratio (for the sake of visual clarity the curves have been offset by a suitable amount). For the most concentrated sample are also shown the position of the maxima and their order. (B) Repeat distance, measured in the L phase as a function of $(\Phi_{w+PC})^{-1}$. Φ_{w+PC} is the sum of water and lecithin volume fractions. Dots denote experimental data (listed in Table 1); the straight line is the best fit according to eq 1.

Table 1. Measured and Calculated Data for the Lamellar Phase in the Lecithin–D₂O–Isooctane

Φ_{PC}	Φ_{w+PC}	$q (\text{\AA}^{-1})^a$	$d (\text{\AA})^b$	$\alpha (\text{\AA}^2)^c$	$^2H \Delta\nu$ (kHz) ^d	PC (wt %)	D ₂ O (wt %)	W_0
0.38	0.43	0.05	126	49		46.6	6.7	5.5
0.47	0.54	0.051	122	40	8.27	55.5	7.8	5.4
0.48	0.53	0.06	105	50		56.1	7.0	4.8
0.58	0.64	0.077	82	53	8.54	65.2	7.3	4.3
0.58	0.64	0.076	82	53	8.61	64.7	8.1	4.8
0.57	0.64	0.071	88	50	9.41	63.8	9.1	5.5
0.68	0.75	0.076	83	45	9.42	73.9	7.9	4.1
0.79	0.87	0.1	63	51	12.29	81.8	9.1	4.3

^a First-order Bragg peak. ^b Repeat distance. ^c PC polarhead area calculated according to eq 1. ^d D₂O quadrupolar splitting.

the lecithin length ($\sim 22 \text{\AA}$)³ and with the low hydration of samples. The polar head area values are essentially independent from the oil loading (Table 1), and their mean value ($47 \pm 4 \text{\AA}^2$) was very close to that found for neat lecithin (no water and no oil added) of the same brand.¹⁸

For lecithin contents comprised between 27% and 60%, water loading induces the coexistence between gel and lamellar phases. In such a case the lamellar structure was inferred only by microscopy with polarized light (see

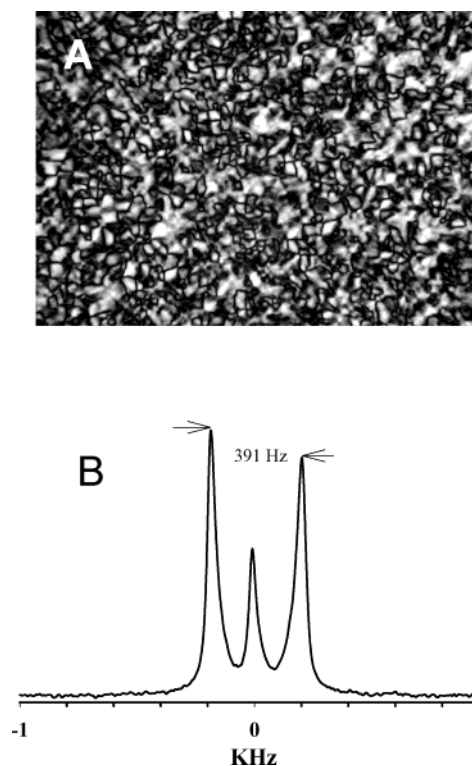


Figure 3. samples in the L_α + gel region of Figure 1. (A) Microphotograph between cross polarizers. Composition: PC = 29%, H₂O = 4%, iC_8 = 67% by weight. (B) 2H NMR spectrum. Composition: PC = 38.2%, D₂O = 4.6%, iC_8 = 57.2% by weight.

Figure 3A) and by 2H NMR quadrupolar splittings (in samples prepared with heavy water; Figure 3B). The equilibrium between the gel and the L_α phase is strongly temperature dependent (with the L_α phase favored at lower temperatures).

Summarizing, starting from binary PC/ iC_8 mixtures the response of the system upon water addition is the following. We found first the gel phase, then the system turns into two phases coexisting in a narrow range of W_0 (3.5–6): a gel and either pure isooctane (at PC < 25 wt %) or a lamellar phase (PC > 25 wt %) depending on the lecithin concentration. For water loading higher than $W_0 = 6$, an additional feature of the phase diagram manifests itself: the spontaneous formation of milky and opaque samples for a water content up to 35 wt % of water. Under the microscope the samples looked like a coarse dispersion of droplets dispersed in a continuous medium (Figure 4A); observation under polarized light reveals the presence of textures associated to lamellar structures, such as oily streaks and maltese crosses (Figure 4B). The emulsion formation is independent from the order of mixing of components and is achieved upon very gentle mixing.²² The emulsion shows a remarkable insensitivity to the temperature: warming the samples up to 70 °C or cooling them down to 4 °C does not induce any appreciable change. Water-soluble dye and microbial cells partition themselves exclusively on the droplets, thus confirming their aqueous nature.²² We note also that the emulsion samples reflect, somehow, the phase equilibria found at lower water loading. In particular, for samples with lecithin contents less than about 20 wt %, a macroscopic separation between the emulsion and pure isooctane is found, reminiscent of the oil + gel equilibrium. On the contrary, for samples with lecithin content higher than 25 wt %, sedimentation of the emulsion is never observed.

Moving along water dilution lines the emulsions disappear for high enough water content. For lecithin concen-

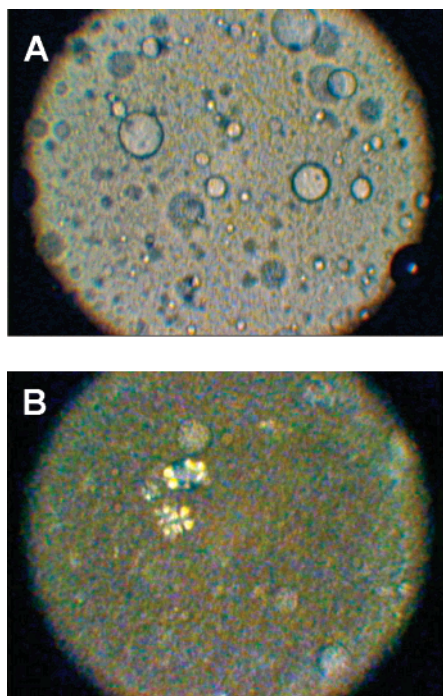


Figure 4. Samples in the emulsion region of Figure 1. Microphotographs with unpolarized light (A) and through cross polarizers (B). Composition: PC = 31.7%, H₂O = 20.9%, iC8 = 47.4% by weight.

trations less than 25 wt %, this happens in a narrow slot of water/PC ratios (around 1/1 by weight) and the system suddenly reveals a classical Winsor II phase separation, with pure water in equilibrium with a low viscous microemulsion rich in oil. The transition from the emulsion to the Winsor II phase separation is gradual in optical appearance: the opaque and viscous emulsion becomes more and more transparent and fluid upon water addition. For very low lecithin concentrations close to the water/isooctane binary axis, a three-phase equilibrium is found. The corners of the triangle are (almost) pure water and isooctane and a microemulsion containing 3.5 wt % of lecithin and 5.2 wt % of water (Winsor III phase separation).

For lecithin concentration higher than 20 wt %, water loading of the emulsion results in a complex coexistence of water with at least two liquid crystalline phases. Samples with PC/iC₈ ratios of 2.2 wt/wt for $W_0 > 50$ show under a polarizing microscope nongeometric striated textures typical for hexagonal lyotropic liquid crystals (Figure 5A). The two-dimensional hexagonal structure was confirmed by the SAXS curve shown in Figure 5B, characterized by broad reflections in the ratio $1:\sqrt{3}:2:\sqrt{7}:3$. The coexistence of this hexagonal phase with pure water is strong evidence of a *reverse* morphology of the aggregates (a direct hexagonal phase almost invariably breaks up into micellar solutions beyond a certain limiting water content).¹⁷ The presence of a *reverse* hexagonal phase in the *same* range of composition was already reported in the case of the systems dioleoylphosphatidylcholine/D₂O/dodecane.¹⁷ For PC/water/isooctane ratios of 22.9/54.3/22.8 (wt), the system shows equilibrium between water and a phase that is optically isotropic and very stiff. The SAXS curve shows the presence of several broad reflections that can be assigned neither to lamellar nor to hexagonal symmetries (not shown). Accordingly this phase is most probably a cubic phase, although the poor quality of the reflections does not permit a safe identification of the space group. Finally, we note that in the region bracketed by

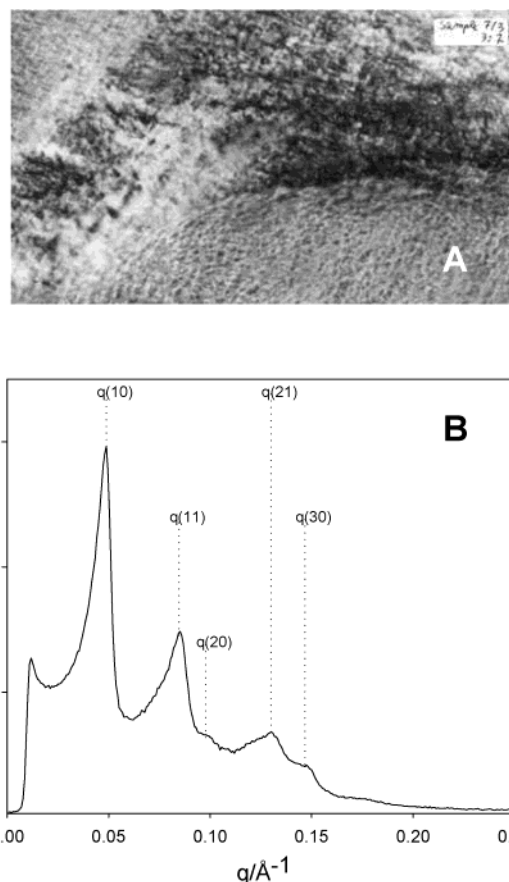


Figure 5. Samples in the H₂ + water region of Figure 1. Composition: PC = 26.1%, H₂O = 62.7%, iC₈ = 11.2% by weight. (A) Microphotograph between cross polarizers. (B) SAXS diffraction pattern. Also shown are the position of the maxima and their order.

0.2–0.45 of lecithin and 0.6–0.3 of water, SAXS reveals a coexistence of water, hexagonal, and another (cubic?) liquid-crystalline phase, but the boundary of this heterogeneous region was not accurately determined.

3.2. PC/Water/iC₈: Long-Time Phase Behavior and Tentative Equilibrium Phase Diagram. After the system ripened of about 1 year, the large region of the phase map that at short time is occupied by emulsions (Figure 1) reveals the complex pattern of phases shown in Figure 6. One year is a very long time compared to the time window of most of scientific activities, but this does not mean necessarily that it is a time long enough to have an equilibrium system. Indeed in Figure 6 are still present some features that are typical of nonequilibrium structures (e.g., spherulites).

Let us start the description from the lecithin–isooctane axis. Increasing the water content, one finds, as in the previous section, first the gel and then the coexistence of gel with pure oil (low PC content) or lamellae (high PC content). Once the two-phase boundaries are crossed, the system shows a *three-phase* equilibrium. Samples reveal the coexistence of a dilute microemulsion, a dense gel, and lamellae separated by flat menisci (a representative sample is also shown in Figure 6). Such a transformation, upon ripening of an opaque emulsion sample into three transparent phases is a strong indication that the system has reached thermodynamic equilibrium. Differences in the mole ratio water/PC among the different phases are within the uncertainty of the NMR method used to determine the composition of the phases. This means that the three-phase triangle is very thin. Actually it was

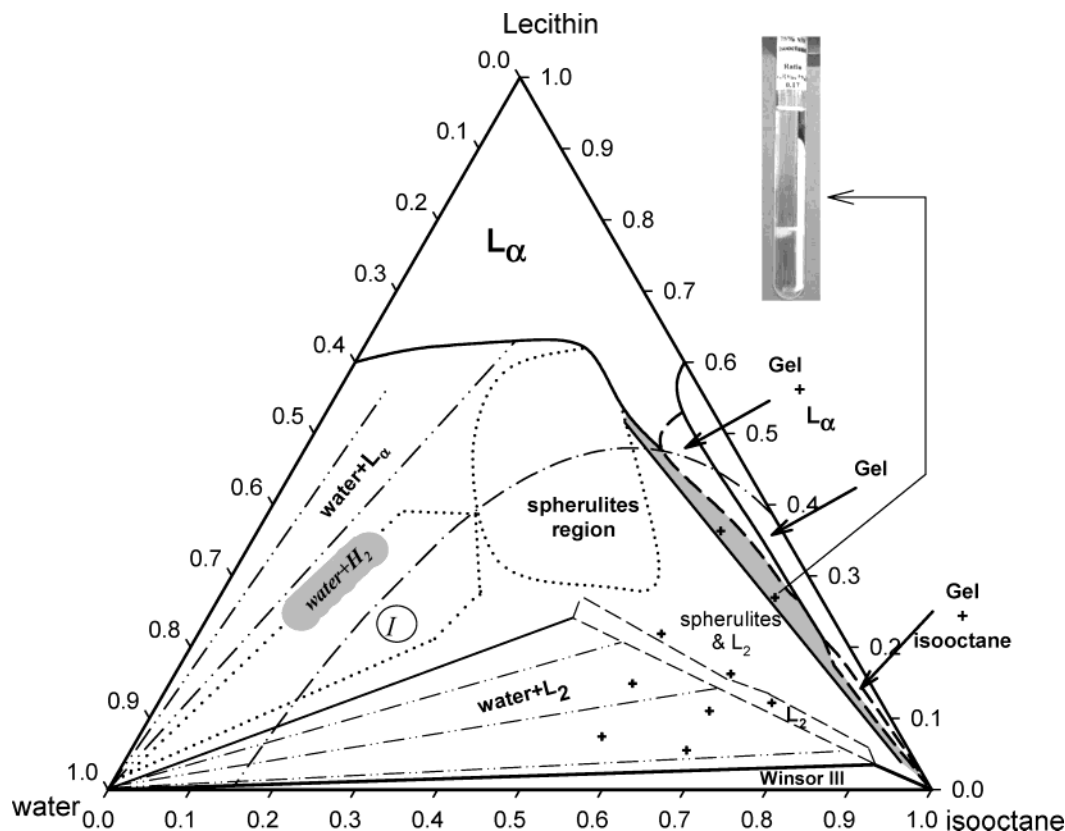


Figure 6. Long time phase map for the system lecithin/water/isooctane (obtained from observations taken after more than 1 year of ripening). Note the three-phase region (in gray) and a representative sample whose location is shown in the inset. The dot-dashed curve denotes the close packing limit for interconnected cylinders according to eq 7. Crosshairs denote the composition of samples listed in Table 2. Other symbols are given in Figure 1.

pictured on the basis of gel/oil and gel/ L_α equilibria, and the two sides of the three-phase triangle correspond to the gel + oil and gel + L_α boundaries already seen in Figure 1. The third side corresponds to an equilibrium between lamellar phase and almost pure iC_8 (strictly a very dilute microemulsion; PC content <0.5%). Such an axis lies along a roughly constant water/lecithin ratio ($W_0 \sim 8-10$). For further water loading the system reveals a two-phase equilibrium between microemulsion and a white precipitate. On heating, the two-phase system turns into a single isotropic phase. On cooling, the phases reappear, in the same proportion. This is in marked contrast with the temperature-insensitivity behavior found for freshly made emulsions sharing the same composition (cf. section 3.1). We take this reversibility upon temperature cycling as an indication that the system is thermodynamically stable. The observation under the microscope of the precipitate reveals that the water droplets have disappeared, and "Maltese crosses" of different dimensions dominate the pattern when viewed through cross polarizers as shown in Figure 7A. A Maltese cross is a texture characteristic of spherulites, i.e., radially oriented microcrystals within a spherical envelope, an arrangement found in materials as dissimilar as polymers, thermotropic liquid crystals, mineral aggregates, and so on. When dealing with surfactant self-assembled structures, spherulite means multilamellar spherical vesicles and can be thought of as an onion-like arrangement of lamellae (indeed, they are also referred to as "onion phase"). Two lines of roughly constant water/lecithin weight ratios define the region of coexistence microemulsion + spherulites: 0.23 ($W_0 \sim 10$) and 1 ($W_0 \sim 47$). In Figure 7B the partition of lecithin between microemulsion and spherulites is shown as a function of the

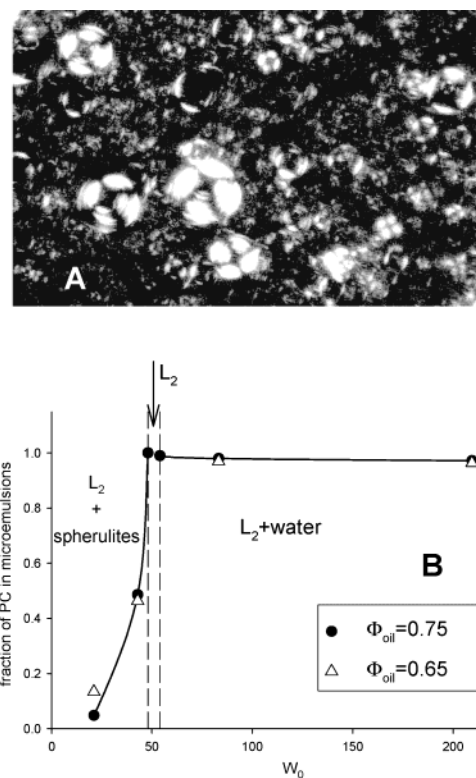


Figure 7. Samples in the L_2 + spherulites region of Figure 6. (A) Microphotograph through cross polarizers of the precipitate. Sample composition: PC = 21.8%, H_2O = 10.7%, iC_8 = 67.5% by weight. (B) Fraction of lecithin in the upper L_2 phase as a function of the overall mole ratio water/lecithin along lines of constant isooctane volume fraction.

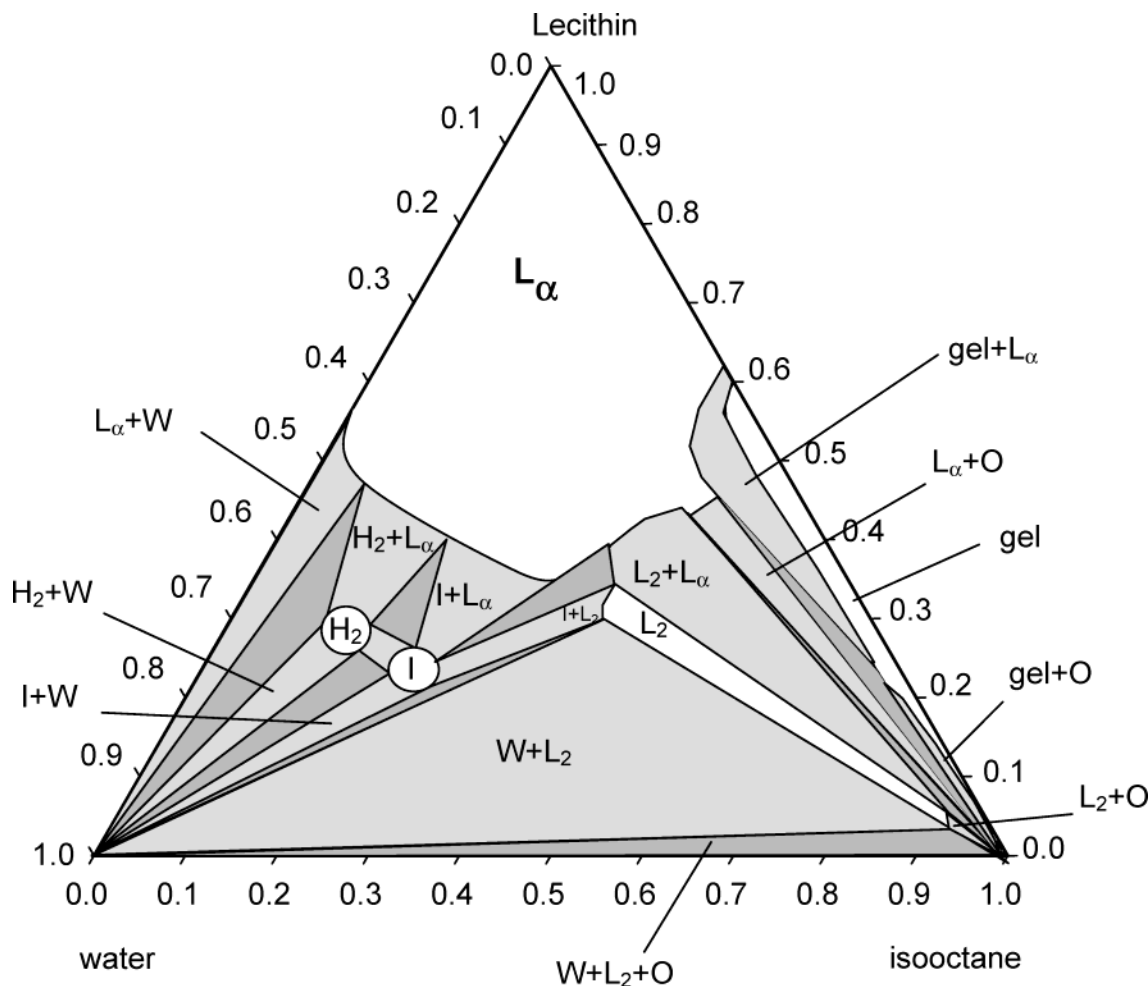


Figure 8. Tentative equilibrium phase diagram for the system lecithin/water/isooctane: single-phase regions in white; two-phase regions in gray; three-phase regions in dark gray. W denotes water and O denotes oil; other symbols are as in Figure 1.

overall water/PC ratio (W_0 seems to be essentially constant in the two phases). Upon water loading the microemulsion becomes more and more concentrated at the expense of spherulites up to $W_0 \sim 47$, where the system turns into a single liquid phase. The range of stability of the single-phase microemulsion upon water loading is very small; the emulsification failure is located along a line of constant $W_0 \sim 54$. For higher water contents the microemulsion expels the excess water resulting in a Winsor II phase equilibrium between reverse micelles ($W_0 \sim 54$) and neat water.

The lecithin content in the microemulsion phase (Figure 7) and the sample composition permit one to map the lower boundary of the region occupied by spherulites (the upper boundary was tentatively drawn according to the extension of emulsions found at short times). However in phospholipid systems, vesicles are almost invariably metastable structures that relax very slowly to a lamellar phase. We feel, therefore, that the region where spherulites were found should be included in the L_α region in a true equilibrium phase diagram. Such a tentative state diagram is drawn in Figure 8 under the assumption that lecithin behaves strictly as a single component and that the overall state diagram obeys the Gibbs phase rule. What we expect is to have two three-phase triangles separated by a two-phase region L_α + oil. The water lean triangle was experimentally found, and it is drawn in the phase map of Figure 6 (L_α + gel + oil). The second triangle is expected at higher water content. Its three sides correspond to the L_α + L_2 , L_2 + oil, L_α + oil equilibria. Since

only the coexistence between L_α and L_2 was found, the other two-phase regions and the three-phase body itself should be very thin. The sequence of phases drawn in Figure 8 is very similar to that found by Kunieda and Shinoda²⁹ for a ternary system with an ethylene oxide based surfactant ($C_{12}E_5$ –decane–water) just above the critical end point (in that system as well, the lamellar phase deeply penetrates into the liquid–liquid closed loop, making the phase behavior very complicated). The presence of a critical end-point around room temperature in the system lecithin–water–isooctane is consistent with the dramatic sensitivity to small temperature changes found in the two-phase regions that equilibrate at short times (L_α + gel and L_2 + oil). Of course one should never forget that lecithin is a multicomponent compound which may complicate the details of the phase diagram.

To conclude this section we report on self-assembly structure of the liquid phases as revealed by NMR self-diffusion experiments.

Lecithin and water diffusion has previously been extensively investigated in samples at $W_0 = 2$ and 3 at various lecithin concentrations,²⁶ so here we recall only the main features. Water and PC molecules experience one-dimensional diffusion along a network formed by branched cylindrical reverse micelles. The observed self-diffusion coefficient depends on the local curvilinear diffusivity and on some features of the network. An upper

(29) Kunieda, H.; Shinoda, K. *J. Dispersion Sci. Technol.* **1982**, *3*, 233

Table 2. Water and Lecithin Diffusivity in Microemulsion (L_2 and Gel) Phases (referred to samples allowed to ripen for more than 1 year; sample compositions are shown in Figure 6 as crosshairs)

sample composition/wt			microemulsion composition			$10^{11} D_w / \text{m}^2 \text{ s}^{-1}$	$10^{11} D_{PC} / \text{m}^2 \text{ s}^{-1}$	$10^{11} D_{w,aq} / \text{m}^2 \text{ s}^{-1}$
% PC	% H ₂ O	appearance ^a	ϕ_o	ϕ_w	W_0			
26.98	5.53	3F	0.88	0.02	9	11.6 ± 0.3	<0.1	10.7 ± 0.3
16.25	16.25	2F	0.81	0.11	54	2.94 ± 0.05	1.52 ± 0.06	2.78 ± 0.04
11.05	21.46	WII	0.82	0.10	54	2.64 ± 0.08	1.97 ± 0.06	2.46 ± 0.06
5.53	26.98	WII	0.90	0.05	40	3.5 ± 0.1	2.78 ± 0.09	3.1 ± 0.1
12.20	13.30	L_2	0.81	0.1	47	3.8 ± 0.1	2.9 ± 0.1	3.7 ± 0.1
36.32	7.44	3F	0.91	0.02	11	10.8 ± 0.3	<0.1	9.8 ± 0.3
21.88	21.88	2F	0.78	0.10	36	2.82 ± 0.04	1.35 ± 0.08	2.7 ± 0.09
14.88	28.88	WII	0.71	0.17	64	2.45 ± 0.08	1.7 ± 0.1	2.36 ± 0.08
7.44	36.32	WII	0.83	0.10	56	3.30 ± 0.14	2.15 ± 0.05	3.12 ± 0.06

^a Key: 3F = three phases, oil + gel + L_2 ; 2F = two phases, L_2 + spherulites; WII = two phases, L_2 + water.

limit to the observed diffusion coefficient is one-third of the lateral diffusion coefficient (the term one-third reflects the facts that one loses two degrees of freedom in performing a one-dimensional motion³⁰). Since the local self-diffusion coefficient of lecithin is $\sim 10^{-12} \text{ m}^2 \text{ s}^{-1}$ and that of water hydrating phospholipid is $\sim 10^{-10} \text{ m}^2 \text{ s}^{-1}$ (see below), the observed difference of 2 orders of magnitude between water and lecithin self-diffusion coefficients (D_w and D_{PC} , respectively) is not surprising.

Note that here the network is formed by cylindrical reverse micelles interconnected by branches and is located in the water-lean region of the phase diagram. Such a system can be described neither in terms of L_2 phase (disconnected reverse micelles) nor in terms of a classical bicontinuous structure (having a low mean curvature of interfacial film). Such a peculiar microstructure is correctly referred to as *dilute highly asymmetric networks*,³¹ but for the sake of shortness, we use in this paper the term *gel phase* (reminiscent of the rheological properties and of the presence of a network).

In Table 2 are listed the water and PC self-diffusion coefficients determined in the other isotropic, liquid phases of Figure 6. Water partitions itself between the aggregates and the isooctane bulk. As a consequence, the measured D_w reflects the motion of the water molecularly dissolved in the oil (with a diffusion coefficient $D_{w,o}$) and the motion of water present in the aqueous core of aggregates (having a diffusion coefficient $D_{w,aq}$). Since in the relevant range of composition the water saturates the isooctane, one can write^{26,32}

$$D_w = \frac{\Phi_o}{\Phi_w} S D_{w,o} + D_{w,aq} \quad (2)$$

where S is the water solubility in iC_8 (in volume fraction) and Φ_o and Φ_w are the volume fractions of iC_8 and water, respectively. The term $S D_{w,o} = (2.1 \pm 0.1) \times 10^{-13} \text{ m}^2 \text{ s}^{-1}$ has been determined previously,²⁶ and one can (through eq 2) subtract the contribution of free water from the measured data, obtaining $D_{w,aq}$ (the correction is below 10% because we are dealing with high concentration samples). Inspection of Table 2 reveals that the water and lecithin diffusion in the low viscous microemulsions in equilibrium with excess water or with spherulites share the same values (around $10^{-11} \text{ m}^2 \text{ s}^{-1}$). The same holds also for the single-phase microemulsion at $W_0 \sim 47$. On this basis we conclude that for the above-mentioned samples the microemulsion phase is composed by disconnected aggregates formed by water and lecithin. So we

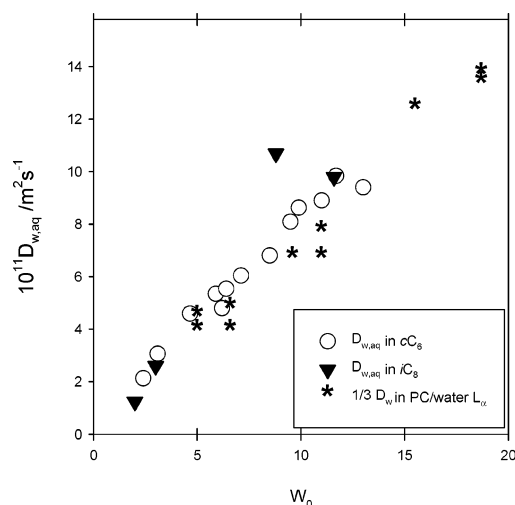


Figure 9. Water self-diffusion coefficient as a function of the lecithin hydration (W_0). The data have been corrected for the contribution of water diffusing in the organic solvent (see text). Triangles refer to the PC/H₂O/ iC_8 system (the data at $W_0 = 2$ and 3 are from ref 26). Circles refer to the PC/H₂O/ cC_6 system (from ref 33). Asterisks indicate one-third of water diffusion measured on oriented lamellae made of water and lecithin (ref 34). The term 1/3 takes into account the different dimensionality of the lamellar system (see text).

are dealing with true L_2 phases. If the self-diffusion coefficients are analyzed under the assumption that the reverse micelles are spherical in shape and behave as hard spheres, one obtains hydrodynamic radii around 150 Å. Such a value is fully consistent with the prediction for spherical, monodisperse reverse micelles made of lecithin and water (cf. eq 4 in section 4.1). At variance the dense isotropic phase found in equilibrium with lamellae and almost neat oil shows different transport properties. Here the PC diffusion is well below $10^{-12} \text{ m}^2 \text{ s}^{-1}$, while water experiences a relatively fast molecular motion ($D_{w,aq} \sim 10^{-10} \text{ m}^2 \text{ s}^{-1}$). Some insight on the microstructure can be gained by plotting $D_{w,aq}$ vs the mole ratio water/lecithin of the microemulsion. This has been done in Figure 9, where we also report the self-diffusion coefficient of water experiencing one-dimensional motion within cylindrical reverse micelles (measured in the PC/H₂O/ cC_6 system),³³ and of water in lamellar phases in the PC/H₂O binary system³⁴ (in this last case we report one-third of the diffusion constant in order to have values relevant to one-dimensional motion).³³ It is evident from Figure 9, that the $D_{w,aq}$ probed in the PC/H₂O/ iC_8 system at $W_0 < 10$

(30) Lindblom, G.; Wennerstrom, H. *Biophys. Chem.* **1977**, *6*, 167.

(31) Tlusty, T.; Safran, S. A.; Strey, R. *Phys. Rev. Lett.* **2000**, *84*, 1244. Tlusty, T.; Safran, S. A. *J. Phys. Condens. Matter* **2000**, *12*, A253.

(32) Skurtveit, R.; Olsson, U. *J. Chem. Phys.* **1992**, *96*, 8640.

(33) Angelico, R.; Balinov, B.; Ceglie, A.; Olsson, U.; Palazzo, G.; Söderman, O. *Langmuir* **1999**, *15*, 1679.

(34) Wassel, S. R. *Biophys. J.* **1996**, *71*, 2724.

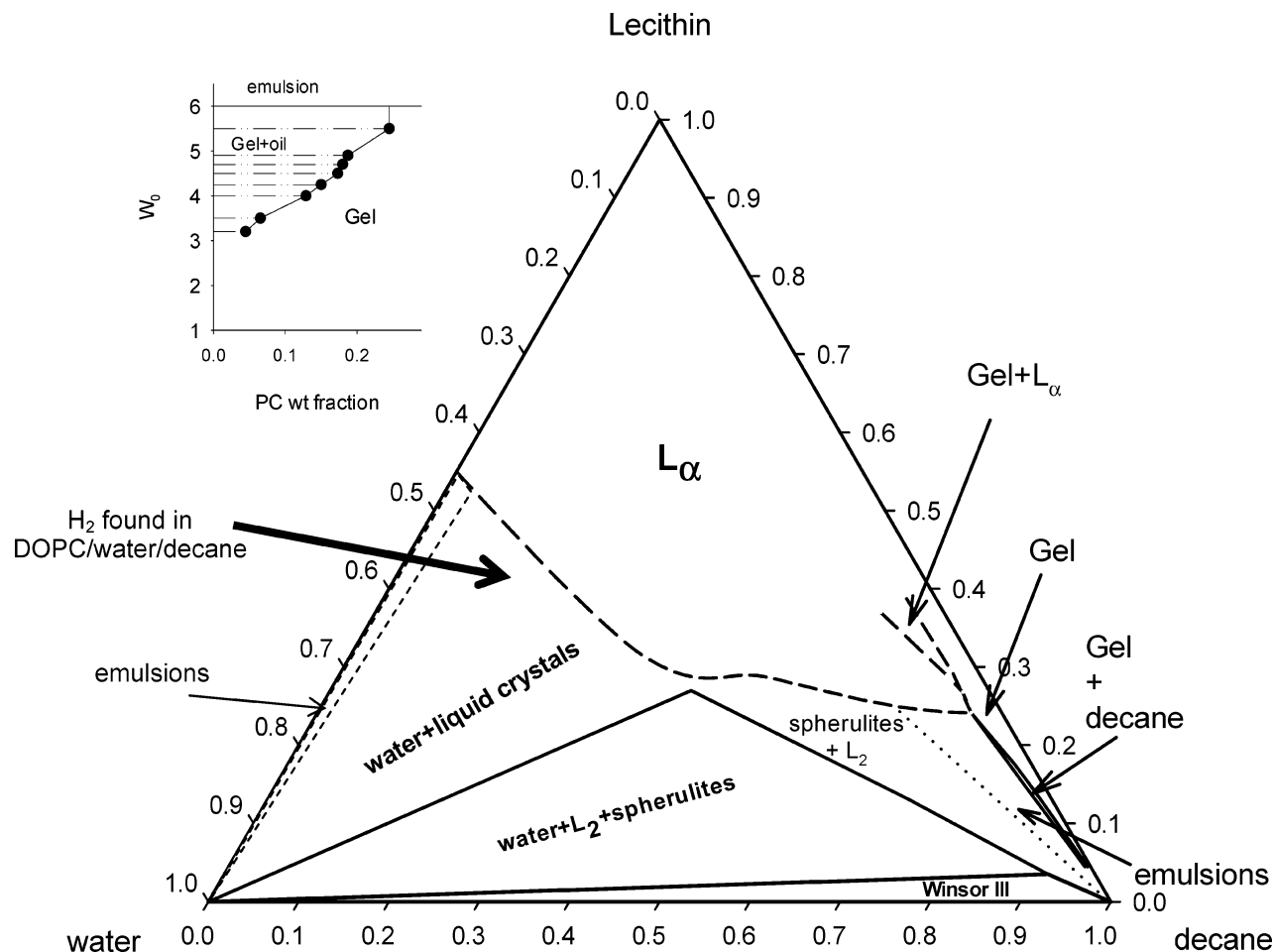


Figure 10. Phase diagram for the system lecithin/water/decane (obtained from observation taken over a time window of 3 months). Note that the full extension of the gel phase and of the L_α + gel region was not determined. The region where the H_2 phase is present was taken from literature.³⁶ Inset: extension of the gel + decane coexistence loop shown as W_0 vs lecithin weight fraction.

follows the trend expected for unidimensional motion inside a pipe formed by lecithin molecules. The observed increase in $D_{w,aq}$ upon increasing the hydration of phosphatidylcholine headgroups is independent from the nature of the oil and is almost the same for water secluded in cylinders and in lamellae when the variation in dimensionality is properly taken into account. Therefore also for the viscous isotropic phase at $W_0 \sim 8$ the microstructure consists of unidimensional water channels surrounded by a lecithin film. The question if these wormlike reverse micelles are branched or not cannot be addressed on the basis of water diffusion data without a detailed study of PC diffusion.²⁶ Indeed, although falling on the same trend, the points at $W_0 = 2$ and 3 in isooctane refer to a branched network, while the data obtained with cC_6 as a solvent refer to disconnected wormlike micelles (strictly a L_2 phase). However, on the basis of the phase equilibrium and of consideration exposed in section 4.1, we can safely label the viscous isotropic phase at $W_0 \sim 8$ as a gel (interconnected micelles).

3.3. PC/Water/Decane Phase Behavior. The addition of a tiny amount of water to lecithin/decane solutions induces a dramatic increase in viscosity, and the resulting organogel shares with the isooctane-based system a complex rheological behavior.¹² Moreover it was reported³⁵ that the PC/water/ C_{10} system, upon addition of excess water, expels pure decane thus undergoing a phase separation (dense gel + oil) similar to that found in the

PC/water/ iC_8 system. To ascertain if such a similarity is fortuitous or extends to the whole phase diagram, we have undertaken the rough determination of the phase map shown in Figure 10. It is based on a limited number of samples (40) equilibrated for less than 3 months, so that this draft reveals some inconsistencies with the Gibbs rule.

Also for the decane-based system, upon water addition one observes first the gel and then the coexistence of gel with pure oil (low PC content) and lamellae (high PC content). The area where the gel coexists with pure oil is similar in size and position in both the isooctane and decane systems (compare the insets of Figures 1 and 10). As in the isooctane case, further water dilution results in the formation of stable emulsions. (We note that with decane stable emulsions are found also very close to the binary PC–water axis.)

A large part of the phase diagram is occupied by a lamellar phase encompassing the regions where L_α and spherulites are present in the PC/ H_2O / iC_8 system. This indicates that with decane as oil infinite lamellae successfully compete with close multilamellar structure. At water loading high enough ($W_0 \sim 52$), excess water coexists with a low viscosity microemulsion (presumably L_2 phase) and with spherulites. We have observed with *isooctane* as oil such a coexistence of reverse micelles, water, and spherulites as an intermediate step in the time course that drives the emulsion (freshly prepared samples) into a stable Winsor II phase separation. Likely, also the phase map of the decane based system is not yet at the

equilibrium, at least for the region denoted as L_α + water + spherulites. The bold arrow in Figure 10 indicates the region where a reverse hexagonal phase was found in a previous study.³⁶ Note that it shares almost the same location on the phase diagram with the H_2 phase found with isooctane (Figure 6); note also that ref 36 deals with pure dioleoylphosphatidylcholine and not with soy bean lecithin.

The multiphasic region close to the decane corner, bracketed by two lines of almost constant W_0 (6 and 52), is very complicated and was not investigated in detail. It consists of emulsions close to the gel + decane area and of equilibria between L_2 and L_α (sometime spherulites) near the water emulsification failure ($W_0 \sim 52$); according to the Gibbs rule, a single-phase L_2 microemulsion is also expected but we have not attempted to map it.

As a whole, Figure 10 reveals a striking similarity with Figures 1 and 6. In particular, the water lean regions are essentially the same with both solvents with almost the same gel + oil area. To corroborate this similarity, extensive rheological studies¹² support the presence of branched micelles in decane as well. For PC contents higher than 25 wt %, the gel coexists with a lamellar phase (although in this case the boundaries of the L_α + gel region have not been determined at high PC content). Interesting, in this region the system shows rheological behavior that obeys a Maxwell model consisting of two elements in parallel with two relaxation times.^{37,38}

4. Discussion

4.1. Guidelines for the Interpretation of the Phase Diagrams. (a) The Flexible Surface Model.^{39,40} In the flexible surface model of microemulsions one focuses on the curvature elasticity of the polar–apolar interface.^{39,40} The relevant length scale in such an approach is the radius of curvature of the interfacial film.

Within the harmonic approximation, the curvature free energy density can be written as⁴¹

$$g_c = 2\kappa(H - H_0)^2 + \bar{\kappa}K \quad (3)$$

Here, H and K are the local mean and Gaussian curvatures of the interface and H_0 is the spontaneous curvature. κ and $\bar{\kappa}$ are the bending rigidity and saddle splay constants, respectively. κ should always be positive, since only in this case the spontaneous curvature is favored. On the contrary, $\bar{\kappa}$ can be either positive or negative; films that prefer isotropic shapes (where the Gaussian curvature is positive) such as spheres will have $\bar{\kappa} < 0$, while films that prefer saddle shapes (where the Gaussian curvature is negative) will have $\bar{\kappa} > 0$. Taking into account the relations $H = R_s^{-1}$ and $K = R_s^{-2}$ valid for a sphere of radius R_s and $H = (2R_c)^{-1}$ and $K = 0$ valid for a cylinder of cross-sectional radius, R_c , one can calculate the relative stability of spherical and cylindrical films.⁴² Here we are mainly concerned with reverse structures and we adopt the convention of counting curvature toward water as positive. For cylinders and spherical droplets, the inner radius is

determined by the conservation of surfactant (total interfacial area of the drop) and of the interior phase

$$R_{wc} = \frac{3(W_0 v_w + v_{hg})}{\alpha} \quad \text{for sphere} \quad (4)$$

$$R_{wc} = \frac{2(W_0 v_w + v_{hg})}{\alpha} \quad \text{for cylinder}$$

where R_{wc} is the radius of the water core containing also the lipid headgroup of volume v_{hg} . Neglecting the entropy contribution, the maximum droplet's size is $R_{wc} = (1 + \bar{\kappa}/2\kappa)/H_0$; for further water addition the system expels excess water leading to a Winsor II equilibrium between excess water and droplets of the optimal size, a situation usually called "emulsification failure". For small values of W_0 ($R_{wc} < 2/3(1 + \bar{\kappa}/2\kappa)/H_0$) cylindrical structures are more stable and wormlike reverse micelles are expected. With increase in the water content, the aggregate structure evolves toward spherical reverse micelles that are always present at the emulsification failure.

(b) Branched Networks.^{31,43,44} When one allows for junctions among aggregates (branches), the above-described model must be modified. A further length scale becomes relevant: the typical distance between branch points.^{31,43} Moreover, also in the absence of any specific interaction between aggregates, the presence of the junctions induces an effective interaggregate attraction (note that the presence of branches results in an attraction between all the micellar parts and not only between branch points).^{31,43} This junction-induced attraction is, for 3-fold branches, strong enough to drive a reentrant phase separation between a dense network and a dilute micellar phase.

The effective intermicellar attraction is governed by the free energies required to form a branch and an end-cap.⁴⁵ The curvature energy of a junction is a nonmonotonic function of the cylinder radius⁴⁵ and so, if we are dealing with water as dispersed phase, of the W_0 (cf. eq 4). As a result, theory foretells (for water-in-oil systems) that the effective attraction between the junctions exhibits a steep maximum at a given W_0 value. Hence, increasing W_0 from the lower side of this maximum increases the effective attraction leading the system to phase separate. A further increase in water content decreases the attraction so the entropy tends to remix the phases. As a whole, the coexistence between a dense network and a dilute micellar phase (sometime referred to as gas–liquid transition) is located within a closed loop with two critical points. Usually, a further increase of the dispersed phase reduces the degree of connectivity until only disconnected cylinders remain and the system behaves as predicted by the flexible surface model of point (a) above. However, under some conditions the emulsification failure boundary enters the loop so that network and excess dispersed phase coexist.^{31,46} A counterintuitive feature of the models describing branched network is that for a high enough concentration the liquid–gas transition disappears (the system demixes at low concentration but is stable at high concentration).⁴⁷

(36) Sjölund, M.; Rilfors, L.; Lindblom, G. *Biochemistry* **1989**, *28*, 1323.

(37) Shchipunov, Yu. A.; Hoffmann, H. *Langmuir* **1999**, *15*, 7108.

(38) Mezzasalma, S. A.; Koper, G. J. M.; Shchipunov, Yu. A. *Langmuir* **2000**, *16*, 10564.

(39) Safran, S. A. *Statistical Thermodynamics of Surfaces, Interfaces and Membrane*; Addison-Wesley Publishing Co.: New York, 1994; Chapter 8.

(40) Olsson, U.; Wennerström, H. *Adv. Colloid Interface Sci.* **1994**, *49*, 113.

(41) Helfrich, W. Z. *Naturforsch.* **1973**, *28c*, 693.

(42) Safran, S. A. *J. Chem. Phys.* **1983**, *78*, 2073.

(43) Zilman, A. G.; Safran, S. A. *Phys. Rev. E* **2002**, *66*, article no. 051107.

(44) Kindt, J. T. *J. Phys. Chem. B* **2002**, *106*, 8223.

(45) Tlustý, T.; Safran, S. A.; Menes, R.; Strey, R. *Phys. Rev. Lett.* **1997**, *78*, 2616.

(46) Bernheim-Groswasser, A.; Tlustý, T.; Safran, S. A.; Talmon, Y. *Langmuir* **1999**, *15*, 5448.

(47) Drye, T. J.; Cates, M. E. *J. Chem. Phys.* **1992**, *96*, 1367.

(c) Packing Constraints.^{48,49} The maximum volume fraction, Φ^{\max} , allowed to hard objects, depends on the type of structure in which they pack. The Φ^{\max} parameter varies with the packing structure:

(i) For hard spheres arranged in cubic, body-centered cubic, and face-centered cubic structures, Φ^{\max} is equal to 0.52, 0.68, and 0.74, respectively. (ii) For disconnected cylinders differing in their arrangements in either hexagonal or square structures, the Φ^{\max} value is 0.91 and 0.78, respectively. (iii) For interconnected cylinders arranged either in cubic or in face-centered cubic structure, Φ^{\max} is 0.94 and 0.82, respectively.^{48,49}

In the present case, the volume occupied by reverse aggregates consists of the sum of the volumes of water, lecithin, and bound oil (the oil taken up in the surfactant tails). The amount of bound oil depends on the surfactant headgroup and on the water content. When the curvature set by the relative amounts of water and surfactant is higher than the spontaneous curvature, most of the volume of the palisade is due to oil "bound" to the surfactant tails. Under such circumstances the volume fraction of the effective packing units exceeds the volume fraction of water and surfactant. It is only when $H = H_0$ that the volume of the packing units coincides with the sum of water and lecithin volumes. On quantitative grounds, the micellar volume fraction is given by^{48,49}

$$\Phi_{\text{mic}} = \Phi_w + \Phi_{\text{PC}} + \Phi_o^b = \Phi_{\text{PC}} \left(1 + \bar{W} + \frac{\Phi_o^b}{\Phi_{\text{PC}}} \right) \leq \Phi^{\max} \quad (5)$$

where Φ_o^b is the amount of bound oil and $\bar{W} = \Phi_w/\Phi_{\text{PC}}$. The ratio $\Phi_o^b/\Phi_{\text{PC}}$ depends on the basic geometry of aggregates and is a function of the W_0 and of the surfactant parameter defined as $s = v_{\text{PC}}/\alpha l_s$ (v_{PC} , α , and l_s are the volume, the headgroup area, and the length of the apolar tail, respectively, of a lecithin molecule).

For spherical reverse micelles, eq 5 becomes

spheres

$$\Phi_{\text{PC}} \left(\bar{W} + \frac{v_{\text{HG}}}{v_{\text{PC}}} \right) \left[1 + \frac{1}{3 \left(\bar{W} + \frac{v_{\text{HG}}}{v_{\text{PC}}} \right) s} \right]^3 \leq \Phi^{\max} \quad (6)$$

while for cylindrical reverse micelles

cylinders

$$\Phi_{\text{PC}} \left(\bar{W} + \frac{v_{\text{HG}}}{v_{\text{PC}}} \right) \left[1 + \frac{1}{2 \left(\bar{W} + \frac{v_{\text{HG}}}{v_{\text{PC}}} \right) s} \right]^2 \leq \Phi^{\max} \quad (7)$$

In a first approximation eq 7 holds for both disconnected and interconnected cylinders as long as the proper value of Φ^{\max} is taken into account; see (ii) and (iii) above.

Ninham and co-workers have previously derived eqs 6 and 7.^{48,49} Here we have simply added the term $v_{\text{HG}}/v_{\text{PC}}$ to take into account for the non-negligible volume occupied by the phosphocholine moiety.

In the calculations we will assume the surfactant parameter of lecithin constant ($s = 1$) and $v_{\text{HG}}/v_{\text{PC}} = 0.162$.

(48) Lisiescki, I.; André, P.; Filankembo, A.; Petit, C.; Tanori, J.; Gulik-Krzywicki, T.; Ninham, B. W.; Pileni, M. P. *J. Phys. Chem. B* **1999**, *103*, 9168.

(49) Lisiescki, I.; André, P.; Filankembo, A.; Petit, C.; Tanori, J.; Gulik-Krzywicki, T.; Ninham, B. W.; Pileni, M. P. *J. Phys. Chem. B* **1999**, *103*, 9176.

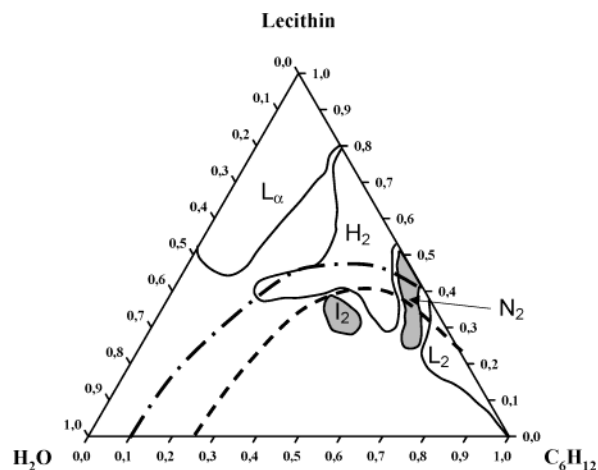


Figure 11. Equilibrium phase diagram of the lecithin/water/cyclohexane system (drawn on the basis of the data of ref 18). Dashed curve denotes the close packing limit for spheres in a face-centered cubic lattice (evaluated according eq 6). Dot-dashed curve is the disconnected cylinders close packing limit (evaluated according eq 7).

We note also that eqs 6 and 7 are derived under the assumption of spheres and cylinders monodispersed in size.

For high enough volume fractions of water and surfactant, the packing constraints dominate the phase behavior. When this is coupled with a composition-dependent surfactant parameter (e.g., when the polar head area strongly depends on hydration), the systems present a complicated pattern of phases. An archetype is the system composed of water, isooctane, and, as surfactant, Cu(II) bis(2-ethylhexyl)sulfosuccinate (CuAOT).^{48,49} In this system upon water loading small spherical reverse micelles are transformed into connected cylinders that in turn are transformed into spherulites (with a lamellar basic geometry) when the relevant close packing limits are crossed.

4.2. Lecithin/Water/Oils Phase Diagrams. The phase diagram for the system lecithin/water/cyclohexane (previously determined by us)¹⁸ is shown in Figure 11 together with the predictions of eq 6 (for spheres in a face-centered cubic lattice) and eq 7 (for a hexagonal array). The L_2 phase closely follows the prediction of the flexible interface model. Indeed, at low W_0 we find *disconnected* cylindrical reverse micelles while at high W_0 the system presents a Winsor II equilibrium between globular reverse micelles and excess water. At intermediate W_0 values (15–19) there is evidence of a coexistence of cylindrical and spherical aggregates (see Discussion in ref 50). The remaining part of the phase diagram can be understood on this basis taking into account the packing constraints upon decreasing the oil content.

For cylindrical micelles the increase in Φ_{mic} induces the classical $L_2 \rightarrow N_2$ (reverse nematic) $\rightarrow H_2$ transition because of excluded volume effects. It is only when Φ_{mic} exceeds to the cylinders close to the packing limit that the aggregates are forced to change themselves into lamellae and the $H_2 \rightarrow L_\alpha$ transition is expected and experimentally found. At *high* W_0 the excluded volume effects drive an ordering of the *spherical* micelles, resulting in the $L_2 \rightarrow$ disconnected cubic (I_2) transition. It should be noted that the I_2 island can be reached from the H_2 phase by increasing the W_0 with a phase transition governed by the curvature energy. However, at the upper limit the

(50) Angelico, R.; Ceglie, A.; Cirkel, P. A.; Colafemmina, A.; Giustini, M.; Palazzo, G. *J. Phys. Chem. B* **1998**, *102*, 2883.

spherical units can occupy on close packing (dashed curve in Figure 11), the aggregates are forced to change their shape first in cylinder and, over the cylinders close packing limit (dot-dashed curve in Figure 11), in lamellae. As a consequence, the H_2 phase strongly protrudes toward the water corner in the phase diagram, separating the cubic from the lamellar phases. As a whole Figure 11 suggests that the lecithin/water/cyclohexane system is governed essentially by the local curvature energy. The larger presence of phases of reverse structure indicates a negative spontaneous curvature, H_0 , of the lipidic film. The absence of bicontinuous intermediate phases suggests a negative value of the Gaussian bending modulus, $\bar{\kappa}$, in agreement with the lack of branched micelles in the L_2 phase.

The situation is very different in the case of isooctane- and decane-based systems. In the following we will discuss explicitly the ternary diagram with isooctane as the oil, but the arguments also should hold for the decane-based system (due to the mutual similarity in phase behavior).

The phase behavior of the PC/ H_2O / iC_8 system reveals clearly some of the features of branched networks. The presence, upon water loading, of gas-liquid transition that disappears for high enough concentration is a peculiarity of self-assembled networks with 3-fold junctions, recognized already on the first treatment of this topic.⁴⁷ Indeed, not only the presence of junctions among micelles has been proved for the gel close the gas-liquid loop, but their branch density was found to scale with PC and water volume fractions as expected for 3-fold branched points.²⁶ However the remaining phase diagram is complicated by a competition between gel and lamellar phases that cannot be accounted for by mere packing considerations. In the phase diagram of Figure 6 the close packing limit for interconnected cylindrical reverse micelles is reported as a dot-dashed curve. Such a boundary successfully secludes the region where the L_α exists as a single phase. However, interconnected cylinders and lamellae coexist well below the close packing limit for interconnected cylinders. The two-phase region between the gel and the lamellar phase is narrow and temperature sensitive. The variation with temperature may be due to temperature dependence of the spontaneous curvature.⁵¹ To summarize, we find that (i) gel and lamellae are separated by a small free energy gap and (ii) lamellae are more stable at higher concentrations and lower temperatures.

On these bases, we can *qualitatively* understand the whole phase behavior of the PC/ H_2O / iC_8 system as follows. The density of junctions was found to increase with W_0 and with the lecithin loading (in agreement with theory). Therefore, at low PC content the system undergoes a gas-liquid transition upon water loading. At the same W_0 but at PC contents > 25%, such a transition is obscured by the gel- L_α transition. For W_0 values higher than about 6, both the effects hold. The dense gel formed upon the gas-liquid transition is so concentrated that it is unstable toward the gel- L_α transition. Such a three-phase body has only a limited extension with respect to water loading, and this likely reflects the reentrant character of the gas-liquid loop (section 4.1.b).

Outside the three-phase body one finds the coexistence of a microemulsion and spherulites (lamellae), a feature already reported for the CuAOT system where it appears when cylinders can no longer pack.^{48,49} An explanation in terms of packing constraints alone does not hold in the PC/ H_2O / iC_8 system, where one finds multilamellar struc-

tures at high dilution as well. One way to understand it is to note that the spontaneous curvature depends on the solvation conditions of the surfactant film. Hence it is expected to depend on the water-to-lecithin ratio before the lecithin headgroups become saturated with water and additional water forms a bulk water pool. Thus, we can have two phases (and composition) in equilibrium (e.g., $L_\alpha + L_2$) where the spontaneous curvature differs. Moreover, because the soybean lecithin is a mixture of different chemical species, preferential partitioning of some compounds between different phases cannot be excluded. What is clear is that upon water loading water and lecithin, molecules move from the lower spherulites phase to the uppermost microemulsion phase (Figure 7B) as found in the CuAOT system^{48,49} as well. The constant $W_0 \sim 52$ represents the boundary for emulsification failure driven by the curvature energy (4.1.a). At the emulsification failure $R_{wc} = (1 + \bar{\kappa}/2\kappa)/H_0$ (section 4.1.a), and under the rough approximation that $\bar{\kappa}$ and κ are the same for lecithin in cC_6 and iC_8 , we have that H_0 in cyclohexane is approximately twice the value in isooctane. This is in agreement with the ability of the oils to penetrate the surfactant tails, which is higher for cyclohexane compared to isooctane.^{52,53} However, in the cC_6 -based system, $\bar{\kappa}$ is likely negative, while the large portion of the PC/ H_2O / iC_8 phase diagram occupied by lamellar or bicontinuous structures suggests for this system that $\bar{\kappa} \approx 0$.

5. Implications

Lecithin solutions in isooctane, cyclohexane, and decane become very viscous upon addition of tiny amounts of water. This fact suggests the systems share a similar microstructure. Such a deduction was confirmed by a number of small-angle neutron scattering studies ascertaining (at least for the cC_6 and iC_8 based systems) that the organogels bear the same *short scale* microstructure: cylindrical reverse micelles.^{3,15,54,55}

The description of microstructure on a longer length scale appears to be much more delicate. The presence of branched networks emerges from rheological¹² and dielectric studies²⁵ (on C_{10} and iC_8 based organogels, respectively). On the contrary, PC and water diffusion indicates in cC_6 the presence of giant disconnected wormlike micelles.^{33,50,56} To complicate the situation, results obtained on a given system have often been used as parameters or assumption in the analysis of data obtained in a different system. Thus it is hard to discriminate if the different microstructures proposed for cC_6 , iC_8 , and C_{10} reflect true differences in the microstructure or are due to the different response of investigation techniques (coupled with an incorrect crossing over of assumption). To have insight on this point, we have undertaken the present phase behavior study.

The determination of phase diagrams is model independent, and the first conclusion that can be drawn by comparing Figures 6, 10, and 11 is unambiguous: the phase behaviors for the iC_8 and C_{10} systems are almost the same and are totally different from that found in the PC/water/cyclohexane (Figure 11). With this in mind, most of the results previously reported appear to be fully

(52) Binks, B. P.; Kellay, H.; Meunier, J. *Europhys. Lett.* **1991**, *16*, 53.

(53) Binks, B. P.; Kellay, H.; Meunier, J. *Phys. Rev. Lett.* **1993**, *70*, 1485.

(54) Schurtenberger, P.; Magid, L. J.; King, S. M.; Lindner, P. J. *Phys. Chem.* **1991**, *95*, 4173.

(55) Jerke, G.; Pedersen, J. S.; Egelhaaf, S. U.; Schurtenberger, P. *Physica B* **1997**, *234-236*, 273.

(56) Angelico, R.; Olsson, U.; Palazzo, G.; Ceglie, A. *Phys. Rev. Lett.* **1998**, *81*, 2823.

(51) Tustly, T.; Safran, S. A.; Strey, R. *Phys. Rev. Lett.* **2000**, *84*, 1244.

consistent. Indeed, evidence of branched networks have been reported for the isooctane (dielectric spectroscopy,²⁵ rheology,⁵⁷ PGSE-NMR²⁶) and decane (rheology)¹² based systems. At variance, the negligible presence of connections between wormlike micelles was reported for the PC/water/cyclohexane system (PGSE-NMR,⁵⁶ dielectric spectroscopy,^{3,58} and light scattering⁵⁹).

Acknowledgment. This work was supported by the MIUR of Italy (PRIN 2001 STRUTTURA E DINAMICA

(57) Cavaco, C. Ph.D. Thesis, ETH Zürich, 1994.

(58) Cirkel, P. A. PhD thesis, Leiden University, 1998; p 81.

DI SISTEMI A GRANDE INTERFASE; PRIN 2003 NANOSCIENZE PER LO SVILUPPO DI NUOVE TECNOLOGIE) and by the Consorzio Interuniversitario per lo sviluppo dei Sistemi a Grande Interfase (CSGI-Firenze). U.O. acknowledges financial support from the Swedish Research Council (VR).

LA035603D

(59) Light scattering results have been successfully analyzed assuming that lecithin in cyclohexane form *disconnected* wormlike micelles. See: Schurtenberger, P.; Cavaco, C. *J. Phys. II* **1993**, *3*, 1279. Schurtenberger, P.; Cavaco, C. *J. Phys. II* **1994**, *4*, 305. Schurtenberger, P.; Cavaco, C. *Langmuir* **1994**, *10*, 100.